Talanta 81 (2010) 1688–1696

Contents lists available at ScienceDirect

Talanta

journal homepage: www.elsevier.com/locate/talanta

Determination of L-ascorbic acid in human serum by chemiluminescence based on hydrogen peroxide–sodium hydrogen carbonate–CdSe/CdS quantum dots system

Hui Chen[a,b], Ruibo Li[a,b], Ling Lin[a], Guangsheng Guo[a], Jin-Ming Lin[b,*]

[a] State Key Laboratory of Chemical Resource Engineering, Beijing University of Chemical Technology, Beijing 100029, China
[b] Analysis Center and Department of Chemistry, Tsinghua University, Beijing 100084, China

ARTICLE INFO

Article history:
Received 5 January 2010
Received in revised form 10 March 2010
Accepted 12 March 2010
Available online 20 March 2010

Keywords:
Chemiluminescence
Flow injection
L-Ascorbic acid
Human serum

ABSTRACT

In the present work, a strongly chemiluminescence (CL) from the mixing of hydrogen peroxide (H_2O_2), hydrogen carbonate (HCO_3^-) and CdSe/CdS quantum dots (QDs) was observed. The addition of trace amount of L-ascorbic acid into the CL system caused significant quenching luminescence intensity. Based on this phenomenon, a flow injection CL analysis system for the determination of L-ascorbic acid was developed. The CL reaction conditions, such as mixing orders and concentrations of CL reagents, flow rates, pH, and particle size of quantum dots have been optimized. The CL intensity and the concentration of L-ascorbic acid have a good linear relationship in the ranges of 1.0×10^{-7}–1.0×10^{-4} mol L^{-1} ($R^2 = 0.9916$). The limit of detection for L-ascorbic acid is 6.7×10^{-9} mol L^{-1} (S/N = 3). This method has been successfully applied to determine L-ascorbic acid in human serum. The recoveries for the real samples were from 83% to 111% and the variance coefficient was <5.3% for intra- and inter-assay precision. A possible mechanism of the CL system was proposed according to results of the kinetic curves of CdSe/CdS QDs in $NaHCO_3$–H_2O_2 CL system, the spectra of CL, fluorescent, UV–visible and ESR. Superoxide ion radical ($^{\bullet}O_2^-$) and hydroxide radical ($^{\bullet}OH$) were generated between the reaction of $NaHCO_3$ and H_2O_2, which were the key intermediates for the production of hole, electron-injected CdSe/CdS QDs and the CL emission.

1. Introduction

L-Ascorbic acid (Vitamin C, AA), with the chemical formula $C_6H_8O_6$, is an important, water-soluble antioxidant in chemical and biological systems. It is existent in fruits and vegetables and indispensable for life, health, physical and daily activity. L-Ascorbic acid is relatively unstable under common storage and processing conditions. Heat, oxygen and transition metals can destroy its structure. It can be synthesized by plants and many mammals, but human cells. In addition, L-Ascorbic acid has an essential role as an enzymatic cofactor for the synthesis of biologically important molecules, such as collagen, carnithine, catecholamine, myelin and neuroendocrine peptides [1], and functions as a free radical scavenger in biological systems by hydrogen atom transfer [2].

Numerous methods have been reported for the determination of L-ascorbic acid. The most common method was titration with an oxidizing agent [3], for example iodate, iodine or N-bromosuccinimide. Spectrophotometric [4], fluorimetric [5], chromatographic [6–8], and electrochemical [9] techniques have also been used to detect L-ascorbic acid. These methods were mainly used to the analysis of pharmaceuticals, fruits and vegetables, few to biological fluids. Furthermore, many shortages such as set up cost, complex extraction, and poor linearity, lack of selectivity or high limit of detection were found in their application. To know the body's L-ascorbic acid status, the content measurement of L-ascorbic acid in blood is very important. Therefore, cheap, sensitive and selective methods, which can provide precise and accurate results, are required.

Chemiluminescence (CL) is a powerful analytical technique with many advantages. The classical oxidants, such as luminol, lucigenin, peroxalate, potassium permanganate and Ce (IV) have been widely developed and employed to applications. CL methods, such as Cu^{2+}–porphyrin–AA system [10], Cr(VI)–luminol–H_2O_2–AA system [11], $KMnO_4$–AA system [12] and hemin–luminol–H_2O_2–AA system [13] have been reported for the detection of AA. But the expensive or poisonous reagent, poor selectivity, narrow linear range or application in tablets mostly cannot achieve good performance. Recently, there were a few of reports about nanoparticles in CL system [14]. Colloidal semiconductor nanocrystals or quantum dots (QDs) have attracted much attention due to their unique size-dependent optical and electronic properties, and have been widely used as multicolored photoluminescent probes [15] and biologi-

* Corresponding author. Tel.: +86 10 62792343; fax: +86 10 62792343.
E-mail address: jmlin@mail.tsinghua.edu.cn (J.-M. Lin).

0039-9140/$ – see front matter © 2010 Elsevier B.V. All rights reserved.
doi:10.1016/j.talanta.2010.03.024

cal luminescent labels [16,17]. The oxidized CL of CdTe QDs/H_2O_2 system and its size-dependent, surfactant-sensitizing effects in aqueous solution have been investigated by Wang et al. [18]. Peroxymonocarbonate ion (HCO_4^-) is a luminous species and can be generated in HCO_3^-–H_2O_2 system [19]. However, the effect of QDs on HCO_4^- has not been reported.

In this work, we present a simple inorganic CL system-$NaHCO_3$–H_2O_2–CdSe/CdS QDs. A strong CL signal was observed when CdSe/CdS QDs was added to $NaHCO_3$–H_2O_2 mixed solution. L-Ascorbic acid can inhibit this CL, and the CL intensity is dependent on L-ascorbic acid concentration. Based on this phenomenon, a new, simple, sensitive and selective method is proposed for the determination of L-ascorbic acid. It has been successfully used to detect L-ascorbic acid in human serum with satisfactory results.

2. Experimental

2.1. Reagents

All chemicals used were of analytical grade. Mercaptoacetic acid (MAA) and hydrogen peroxide (H_2O_2, 30%) were obtained from Alfa Aesar-A Johnson Matthey Company (Heysham, UK). Sodium hydrogen carbonate ($NaHCO_3$), cadmium chloride ($CdCl_2$), sodium sulfide, selenium, L-ascorbic acid (AA) and stearic acid were from Beijing Chemical Reagent Co. (Beijing, China). Sodium borohydride was from Tianjin Chemical Reagent Co. (Tianjin, China). Glycine, D-glucose, isoleucine, aspartic acid and glutamic acid were from Beijing Dingguo Reagent Co. (Beijing, China). L-Cysteine was purchased from Shanghai Chemical Reagent Co. (Shanghai, China). 3-Hydroxytyramine hydrochloride was from Fluka (St. Louis, USA). 5,5-Dimethyl-1-pyrroline N-oxide (DMPO) was bought from Tokyo Kasei Kogyo Co. Ltd (Tokyo, Japan). 2,2,6,6-Tetramethyl-4-piperidine was from Sigma–Aldrich (St. Louis, USA). Human serum samples were obtained from Beijing Chemclin Biotech Co., Ltd (Beijing, China). The water used in the experiments was freshly deionized using an ultraviolet ultrapurewater system (18.3 MΩ cm, Barnstead, IO, USA).

2.2. Apparatus

Batch chemiluminescence experiments were carried with a BPCL luminescence analyzer (Institute of Biophysics, Chinese Academy of Sciences, Beijing, China). The flow injection CL signal was measured with a LumiFlow LF-800 detector (NITI-ON, Funabashi, Japan) with four peristaltic pumps (SJ-1211, Atto, Tokyo, Japan). A centrifuge was employed for sample pretreatment (5804R, Eppendorf, Hamburg, Germany). Absorption spectra were collected by a UV–Vis spectrophotometer (UV-3900, Hitachi, Japan). Emission spectra were measured with a fluorescence spectrophotometer (F-7000, Hitachi, Japan). Electron spin resonance (ESR) spectra were measured on a Bruker spectrometer (ESP-300 E, Bruker, Germany). The mass spectrum was obtained by a Bruker micrOTOF-Q mass spectrometer in negative mode (Bruker Daltonics, Billerica, MA). Fourier transform infrared (FT-IR) spectra were recorded on a PerkinElmer 100 FT-IR spectrometer (Massachusetts, USA). Transmission electron microscopy (TEM) images were recorded by a JEM-1200EX electron microscope operating at 100 kV (JEOL, Japan).

2.3. Synthesis of CdSe/CdS quantum dots

Firstly, colloidal CdSe QDs was prepared using the reaction between Cd^{2+} and NaHSe solution according to the approach described in Ref. [20]. NaHSe solution was obtained by the reaction of selenium and sodium borohydride. CdSe QDs was synthesized by adding freshly prepared NaHSe solution to N_2-saturated $CdCl_2$ solution at pH 11.3 in the presence of mercaptoacetic acid (MAA) as a stabilizer (Reactions 1–2). The molar ratio of Cd^{2+}/MAA/HSe^- was fixed at 1:2.4:0.5. The precursors were converted to CdSe nanocrystals by refluxing the reaction mixture for 3 min at 90 °C under open-air conditions with condenser attached. Then Na_2S solution was added slowly before further refluxing for 0.5–3 h at 90 °C. The molar ratio between Se and S was controlled to be 1:1. The samples collected were then dialyzed against doubly distilled water for 5 h to remove excessive MAA. The final solution was stable for 3 months when stored in a refrigerator at 4 °C.

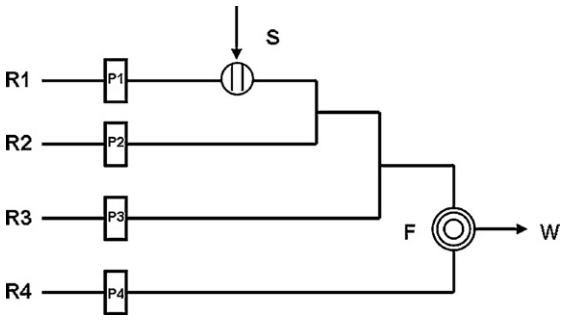

Fig. 1. Schematic diagram for chemiluminescent detection by flow injection system. R1–R4, flow lines; P1, P2, P3, and P4, peristaltic pumps; S, sample injector; F, flow cell; W, waste. Optimal operation conditions: R1, carrier water at 1.5 mL min^{-1}; R2, 0.5 mol L^{-1} $NaHCO_3$ at 1.0 mL min^{-1}; R3, CdSe/CdS QDs at 1.0 mL min^{-1}; R4, 0.5 mol L^{-1} H_2O_2 at 1.0 mL min^{-1}.

$$4NaBH_4 + 2Se + 7H_2O \rightarrow 2NaHSe + Na_2B_4O_7 + 14H_2 \quad (1)$$

$$CdCl_2 + NaHSe + NaOH \rightarrow CdSe + 2NaCl + H_2O \quad (2)$$

2.4. Sample preparation

Human serum samples were kept frozen and stored in dark before experiments. L-Ascorbic acid can be oxidized to diketogulonic acid in the presence of oxygen to interfere with the determination. Fresh serum sample should be used in the detection. They were diluted by metaphosphoric acid in volume ratio of 1:2 and centrifuged at 4000 rpm for 10 min at 4 °C. The supernatant solution was filtrated by 0.22 μm microfilm before detection. For mass analysis, the pretreated sample was diluted by methanol in the same volume.

2.5. Procedure

Light-producing reactions were carried out in the glass cuvette by a batch method and the detection was performed on a BPCL luminescence analyzer. 100 μL carbonate/bicarbonate solution was added to 100 μL CdSe/CdS quantum dots in a cuvette firstly, then 100 μL L-ascorbic acid was injected before the injection of H_2O_2 solution. The CL intensity was displayed and integrated for 0.1 s interval at −1.2 kV.

In flow injection analysis system (FIA), the flow rates of R1, R2, R3, and R4 were 1.5, 1.0, 1.0, and 1.0 mL min^{-1} for the carrier, $NaHCO_3$, CdSe/CdS QDs, and H_2O_2, respectively. 100 μL ascorbic acid standard solution or sample solution was injected into the carrier (H_2O) stream of the flow line R1 by a loop valve injecter, which mixed with the $NaHCO_3$ solution in flow line R2 through a three-way piece. CdSe/CdS QDs solution in flow line R3 mixed with the AA–$NaHCO_3$ solution by another three-way piece. Finally H_2O_2 in flow line R4 mixed with the mixed solution of AA–$NaHCO_3$–CdSe/CdS QDs in a spiral flow CL cell, which was placed in front of the photomultiplier tube. The CL intensity was recorded as the peak height (Fig. 1).

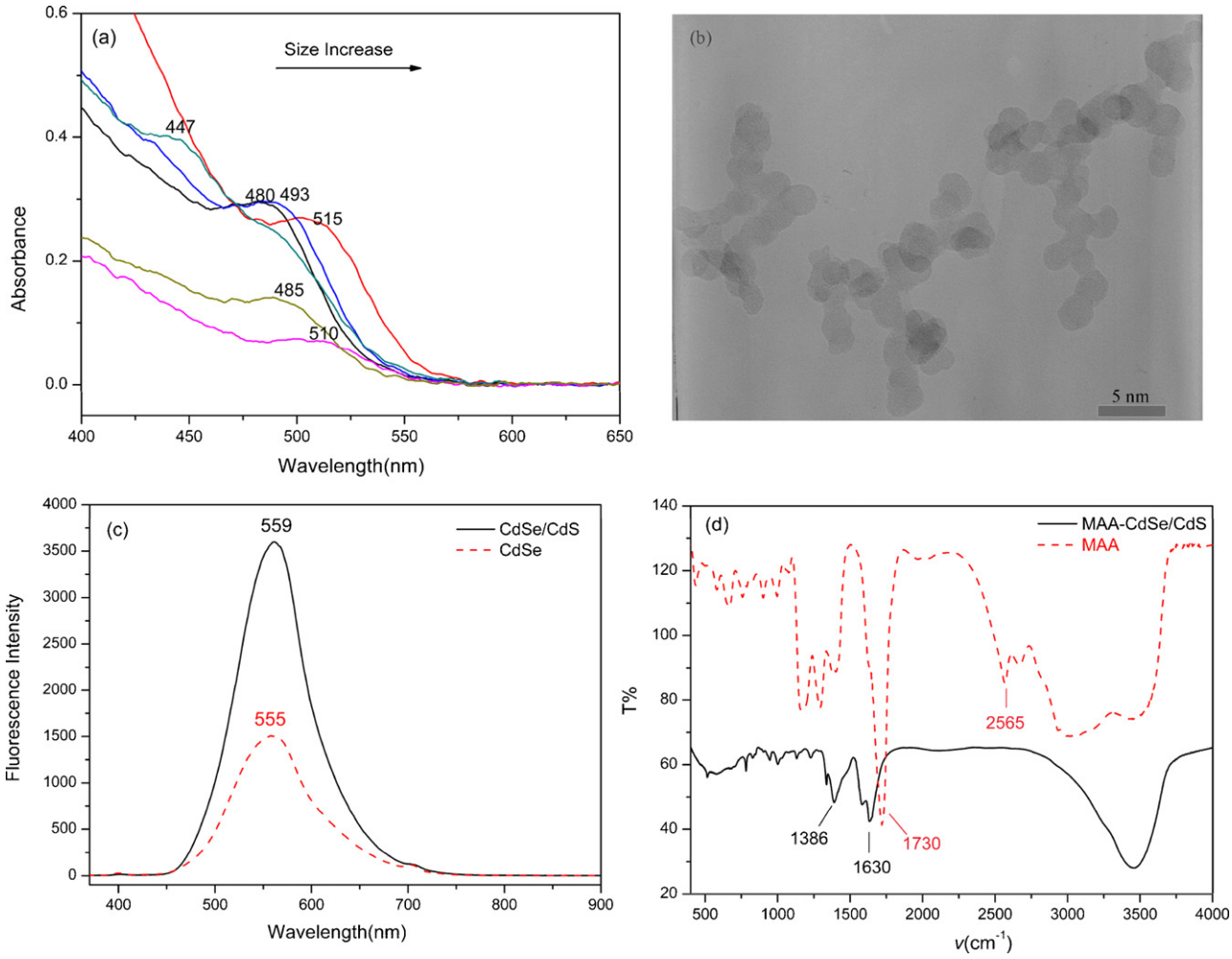

Fig. 2. Characterization of CdSe/CdS QDs. UV–Vis absorption of MAA-capped CdSe/CdS QDs obtained with different heating times. The absorption peaks occur at 447, 480, 485, 493, 510, and 515 nm for the heating times of 0.5, 1.0, 1.5, 2.0, 2.5, and 3 h in the synthesis of CdSe/CdS QDs, respectively. (a) TEM image of CdSe/CdS QDs, (b) fluorescence spectra of CdSe and CdSe/CdS QDs at the same concentration (excited at 350 nm) (c), and FT-IR spectra of MAA and MAA-capped CdSe/CdS QDs (d).

3. Results and discussion

3.1. Characterization of CdSe/CdS QDs

Fig. 2a showed the typical absorption of CdSe/CdS nanocrystals. All samples showed a well-resolved absorption maximum of the first electronic transition, indicating a sufficiently narrow size distribution of the CdSe/CdS QDs. The particle size of synthesized QDs was calculated in virtue of the following expression (Eq. (1′)) [21]:

$$D = (9.8127 \times 10^{-7})\lambda^3 - (1.7147 \times 10^{-3})\lambda^2 + 1.0064\lambda - 194.84 \quad (1')$$

where D (nm) was the size of a given nanocrystal, and λ (nm) was the wavelength of the first excitonic absorption peak of the corresponding nanocrystal. The average size of QDs was about 2 nm. Fig. 2b shows the typical TEM image of CdSe/CdS QDs. The deposition of CdS shell on the CdSe cores resulted in a uniform size distribution.

Room-temperature fluorescence spectra were shown in Fig. 2c. The position of the fluorescent maximum of CdSe QDs was located at 555 nm, whereas CdSe/CdS nanocrystals obtained emit with a fluorescent maximum at 559 nm. The intensity of CdSe/CdS nanocrystals was much stronger than that of CdSe QDs, and the emission spectrum of CdSe/CdS QDs was narrow and symmetrical compared to CdSe QDs. The slight red shift is probably resulted from the passivation of CdSe surface defects by CdS QDs, which leading to the localization of photoexcited charge carriers in the CdSe core [22].

The room-temperature photoluminescence (PL) quantum efficiency (QE) of as-synthesized CdSe and CdSe/CdS QDs nanocrystals were estimated following the procedure of Ref. [23] by comparison with Rhodamine 6G in ethanol assuming its PL QE as 95%. Coating a CdS shell on the CdSe core greatly increased the QE of original CdSe QDs. The calculated PL QE of CdSe and CdSe/CdS were 0.23 and 0.36, respectively.

FT-IR spectrum of MAA showed a peak at 2565 cm^{-1} for stretch vibration of the S–H bond. The diminishment of this peak in the spectrum of 2.14 nm CdSe/CdS QDs (Fig. 2d) indicated the formation of S–Cd bonds between MAA and CdS shell. The shift of the asymmetric vibration of the carboxyl group in MAA from 1730 to 1630 cm^{-1} in these spectra implied that the COOH in MAA turned to its anion, which also led to the appearance of the symmetric vibration of the carboxyl anion at 1386 cm^{-1} in alkali aqueous solution due to the p*K*a values of about 5.2 [24] and 6.1 [25] for MAA. On the basis of above results, structure of the obtained QDs could be identified as a cadmium-rich CdSe core and CdS shell covered with excess MAA^{2-} anions.

Table 1
Effect of mixing order of reagents on the batch CL intensity.[a].

Reagent	Injection	Intensity (count)	Profile
$NaHCO_3$	H_2O_2	225 → 30	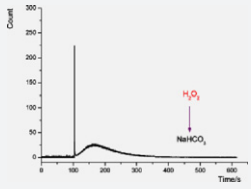
$NaHCO_3$ + QDs	H_2O_2	32,350	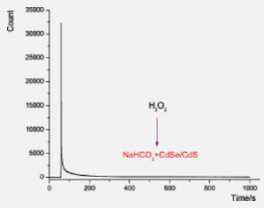
H_2O_2 + QDs + AA	$NaHCO_3$	0	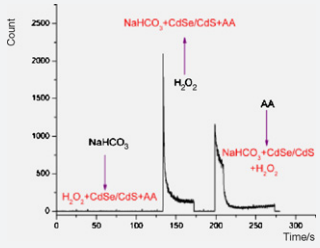
$NaHCO_3$ + AA + QDs	H_2O_2	2092	
$NaHCO_3$ + H_2O_2 + QDs	AA	1154	

[a] $NaHCO_3$: 1.0 mol L^{-1}; H_2O_2: 0.5 mol L^{-1}; QDs: 6.0×10^{-6} mol L^{-1}; AA: 1.0 μmol L^{-1}; injection volume: 100 μL.

3.2. Mixing order of reagents

Mixing order of the reagent solution plays an important role in the light emission. It was examined by batch method using the reaction of $NaHCO_3$, H_2O_2, CdSe/CdS QDs, and L-ascorbic acid. Three different mixing orders were compared in Table 1. It showed that the injection of H_2O_2 solution to $NaHCO_3$ solution provided only a weak CL emission. The injection of H_2O_2 solution into the $NaHCO_3$–CdSe/CdS QDs-AA mixed solution generated the strongest CL emission. Kinetic characteristics were shown in the results obtained by the batch method in Table 1. Two CL peaks were obtained in H_2O_2–$NaHCO_3$ system. The intensity got first maximum value of 225 in 0.2 s, then quenched quickly. After 60 s the second maximum value of 30 was recorded and the CL remained for about 90 s. When QDs was added into H_2O_2–$NaHCO_3$ system, a significant enhancement in the CL signal was observed. About 140 times increased in the CL intensity was obtained in the presence of CdSe/CdS QDs. The curve changed to one CL peak. The CL intensity obtained the maximum value rapidly. The light remained for 500 s before quenched utterly. The CL intensity and lifetime were obviously enhanced. Therefore, the flow injection system was designed as shown in Fig. 1. 100 μL of ascorbic acid solution was injected into the carrier (H_2O) stream of the flow line R1 and the sample was mixed with the $NaHCO_3$ solution of the flow line R2. Then, reagents of these two lines mixed with the CdSe/CdS QDs solution through the flow line R3. In order to obtain a high CL signal and a low CL noise, the H_2O_2 solution in line R4 and the $NaHCO_3$–CdSe/CdS QDs-AA solution were transported separately and mixed inside the flow cell.

3.3. Flow rates of reagents

The flow rates of R1, R2, R3, and R4 will affect the peak height and S/N ratio of AA determination. The peak height increased with the increasing flow rates of R2, R3, and R4, but the noise was also increased. On the other hand, the peak height decreased with an increase of the flow rate of carrier (R1), but the peak shape broadened and a longer analysis time was necessary when decreased the flow rate of R1. After serious optimization, the optimal flow rates of R1, R2, R3, and R4 were 1.5, 1.0, 1.0, and 1.0 mL min^{-1} for the carrier, $NaHCO_3$, CdSe/CdS QDs, and H_2O_2, respectively. Under these conditions, the flow injection CL signals with sharp peaks and relatively low noise for AA were obtained as shown in Fig. 3.

3.4. Optimization of the reaction conditions

The CL intensity and the shape of the kinetic profile were greatly affected by the reaction pH. Experiments in different pH were per-

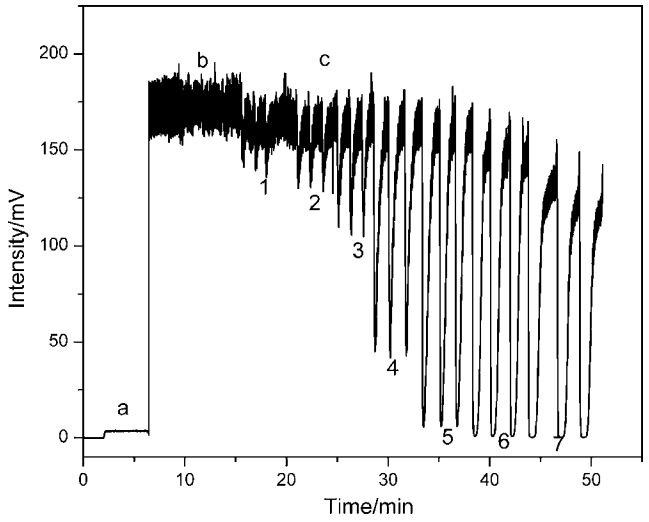

Fig. 3. Typical FIA signals for the determination of AA. (a) Intensity of $NaHCO_3$–H_2O_2 system. (b) Intensity of $NaHCO_3$–H_2O_2–CdSe/CdS QDs system. (c) Intensity of $NaHCO_3$–H_2O_2–CdSe/CdS QDs-AA system. Conditions: concentration of AA (μmol L^{-1}) (1) 0.1; (2) 0.5; (3) 1.0; (4) 5.0; (5) 10.0; (6) 50.0; (7) 100.0. Other conditions as in Fig. 1.

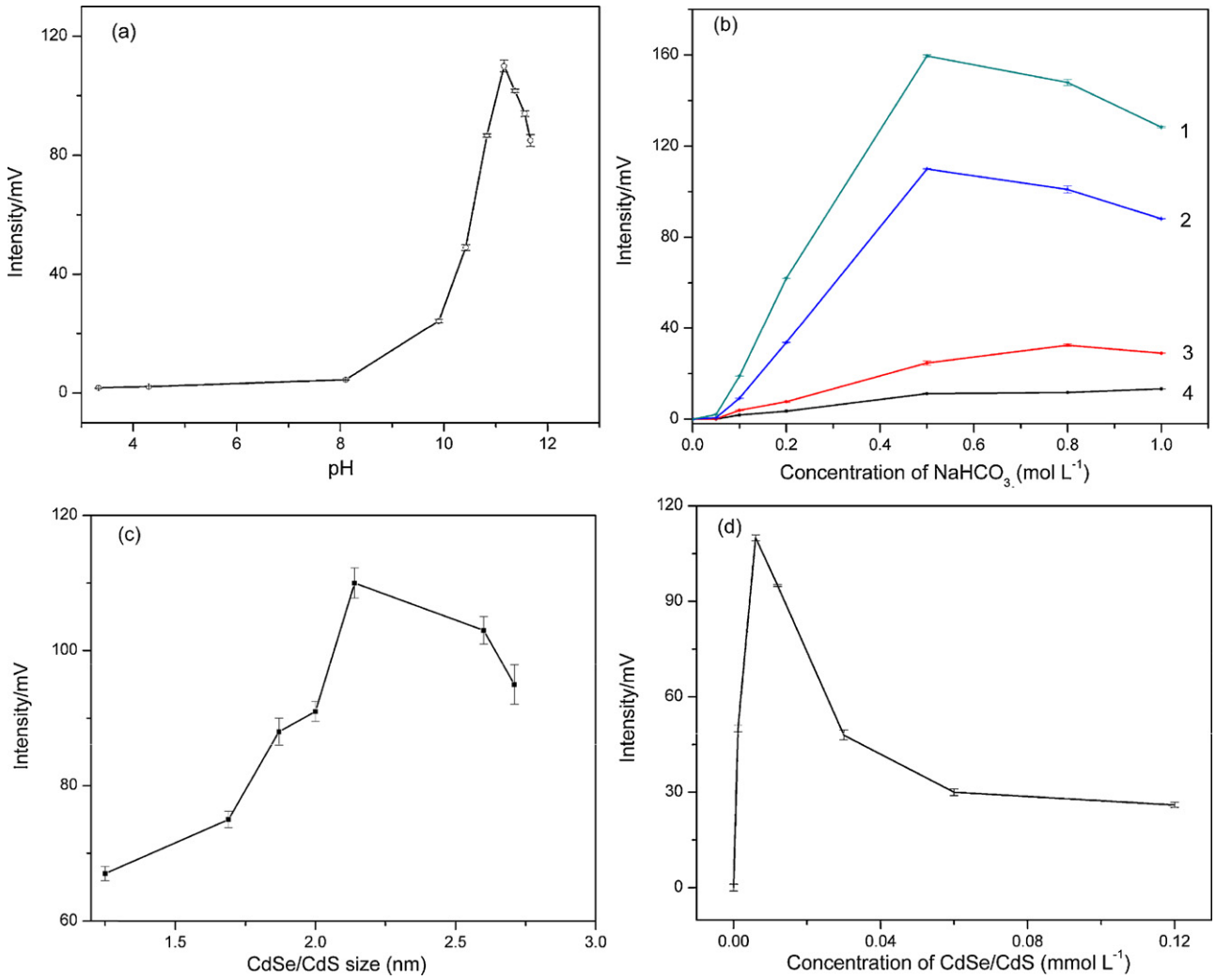

Fig. 4. Effects of pH (a), concentration of $NaHCO_3$: (1) 0.05 mol L^{-1} H_2O_2; (2) 0.2 mol L^{-1} H_2O_2; (3) 0.5 mol L^{-1} H_2O_2; and (4) 1.0 mol L^{-1} H_2O_2 (b), sizes (c) and concentration of CdSe/CdS QDs (d) on the chemiluminescence emission intensity in FIA system. Different pH values were achieved by varying the ratio of 0.1 mol L^{-1} $NaHCO_3$, Na_2CO_3, and 1.0 mol L^{-1} NaOH.

formed, which were achieved by varying the ratio of 0.1 mol L^{-1} $NaHCO_3$, Na_2CO_3, and 1.0 mol L^{-1} NaOH. As shown in Fig. 4a, the CL intensity was increased with increasing pH value, reached a maximum at 11.16. With the increase of pH, the CL system contained more OH^-, the CdSe/CdS QDs surface was more negatively charged, and the electron transfer from the conduction band of CdSe/CdS QDs was easier. Furthermore, $^{\bullet}O_2^-$ species is more stable in high pH solution benefiting to the CL emission and leading to the increasing CL intensity. But when the pH was higher than 11.16, too many anions loaded on the surface of CdSe/CdS QDs, which would suppress the approach of negatively charged $^{\bullet}O_2^-$ to the CdSe/CdS QDs surface, and make the decrease of CL intensity. When 1.0 mol L^{-1} or a higher concentration of NaOH was added, the CL emission was totally quenched. Therefore, the pH value of 11.16 was selected in this CL system.

The effect of the concentration of $NaHCO_3$ was examined. As shown in Fig. 4b, the maximal response was obtained at about 0.5–0.8 mol L^{-1}. The solubility of $NaHCO_3$ in water was limited and a concentration of 0.5 mol L^{-1} $NaHCO_3$ was chosen as the most convenient one for the following experiments. The concentration of H_2O_2 played an important role in the CL reaction. H_2O_2 reacted with $NaHCO_3$ to generate HCO_4^- ions leading to the formation of $^{\bullet}OH$ radical. Simultaneously, H_2O_2 reacted with the reactive intermediate and yielded $^{\bullet}O_2^-$ radicals. Excessively low concentration of H_2O_2 cannot yield enough HCO_4^- ions, but too high concentration H_2O_2 can cause rapid decomposition producing air bubbles in the reaction which will affect the system light emitting and stability. The CL intensity for four different concentrations of H_2O_2 in the range of 0.05–1.0 mol L^{-1} increased on increasing the concentration of $NaHCO_3$, but the background and noise became significantly higher. The concentration of 0.5 mol L^{-1} was selected for subsequent investigation.

Size effect is a basic characteristic of semiconductor nanocrystals. It was found that the CL intensity gradually increased with the increase of particle size of CdSe/CdS QDs. Fig. 4c showed that the highest CL intensity was obtained by the CdSe/CdS QDs with 2.14 nm in diameter. According to CL energy match theory, the energy band gap of semiconductor QDs decreased with the increasing particle size. The CL intensity increased with the decreasing band gaps, which lead to a faster electron injection to the surface states of QDs. But when QDs were larger than 2.14 nm in diameter, the CL intensity decreased with the increasing size. It would be due to the relative small surface-to-volume ratio, leading to the injection of electrons to the surface states of small QD particle become more difficult.

Different concentrations of CdSe/CdS QDs were added to the CL system, they enhanced the CL intensity in different degree (Fig. 4d). The CL intensity can be gradually intensified when the concentration of CdSe/CdS QDs is lower than 6.0×10^{-6} mol L^{-1}.

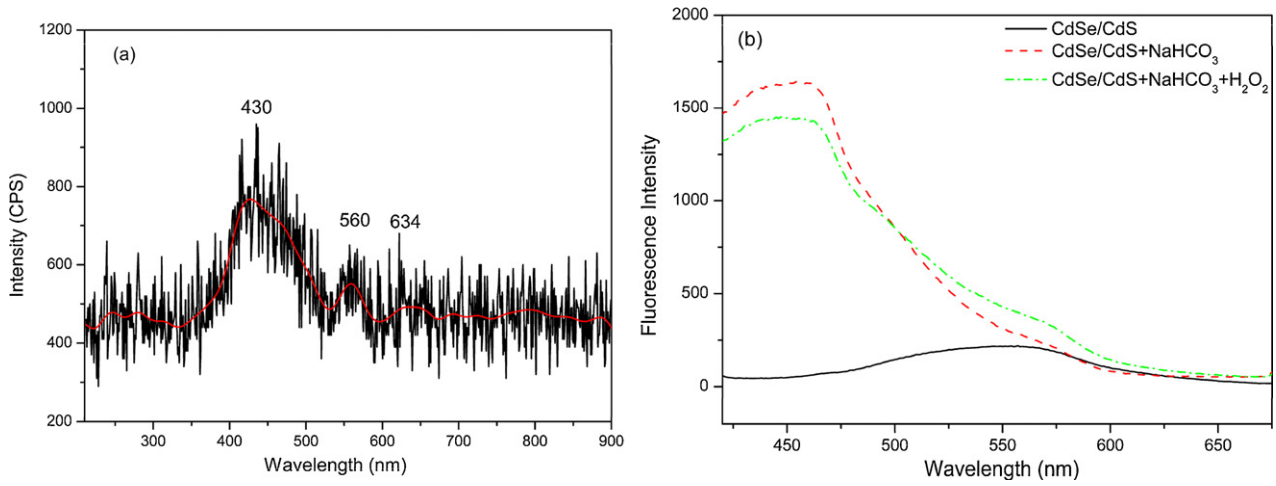

Fig. 5. Emission spectra of $NaHCO_3$–H_2O_2–CdSe/CdS QDs CL systems (a), and fluorescence spectra of $NaHCO_3$–H_2O_2–CdSe/CdS QDs system before and after reaction (b).

The energy generated during the chemical reaction between H_2O_2 and $NaHCO_3$ was limited. It can excite a certain amount of CdSe/CdS QDs. When the concentration of CdSe/CdS QDs was more than 6.0×10^{-6} mol L^{-1}, the chemical energy cannot satisfy the distribution to all QDs. The CL efficiency was affected. Furthermore the CdSe/CdS QDs molecule collision chance was increased in the dense reactive solution and the light quenching was enhanced. Therefore, the CL intensity was decreased. The CdSe/CdS QDs of 2.14 nm at the concentration of 6.0×10^{-6} mol L^{-1} gave the most sensitive response and were selected as the CL enhancer in this study.

3.5. CL and fluorescent spectra of CL systems

CL spectrum from the reaction of $NaHCO_3$–H_2O_2 and CdSe/CdS QDs detected by flow system was shown in Fig. 5a. Three peaks located at 430 nm, 550 nm and 634 nm, were observed. Peak at 430 nm corresponded to the decomposition of excited double $(CO_2)_2$* [26]. The decomposition energy of $(CO_2)_2$ dimer was calculated by the EHMO method and found to be 132 kcal mol L^{-1}, which was high enough to promote emission at a wavelength higher than 220 nm [27]. Peak at 634 nm resulted from the emission spectra of $^1O_2$ [28,29]. They have higher energy and can lose excess energy by luminescence. Peak at 560 nm showed the similar emission peak position of CdSe/CdS QDs, which indicated that the emitter of the CL emission was the excited state of QDs.

Fluorescence spectra of CdSe/CdS QDs, the mixture of $NaHCO_3$–CdSe/CdS QDs, and the mixture of $NaHCO_3$–H_2O_2–CdSe/CdS QDs were recorded in Fig. 5b. It was found that fluorescence peak of CdSe/CdS QDs at 559 nm was the same before and after the reaction. CdSe/CdS QDs did not vanish during the reaction. They only enhanced the fluorescence emission intensity and did not influence the fluorescence spectra. It further confirmed that CdSe/CdS QDs was the luminant of the CL system.

3.6. Mechanism of the CL system

It was reported that peroxymonocarbonate ion (HCO_4^-) was yielded in bicarbonate and H_2O_2 system [30]. The correlated research about HCO_3^-–H_2O_2 system was given in detail by our group [31–34]. Superoxide ion radical ($^\bullet O_2^-$) and hydroxide radical ($^\bullet$OH) were generated in H_2O_2–$NaHCO_3$–CdSe/CdS system and were the key species in CL emission. The products of the simultaneous processes of decomposition and radical recombination were molecules of $^1O_2$ and $(CO_2)_2$* [35,36], which released the excess energy immediately and produced CL emission [37]. $^\bullet O_2^-$ can easily donate one electron to the 1Se quantum-confined orbital of CdSe/CdS QDs to form electron injected CdSe/CdS (e^-_{1Se}) QDs. At the same time, $^\bullet$OH ions injected a hole in the 1Sh quantum-confined orbital of CdSe/CdS QDs to form hole injected CdSe/CdS (h^+_{1Sh}) QDs. An electron-transfer reaction between CdSe/CdS

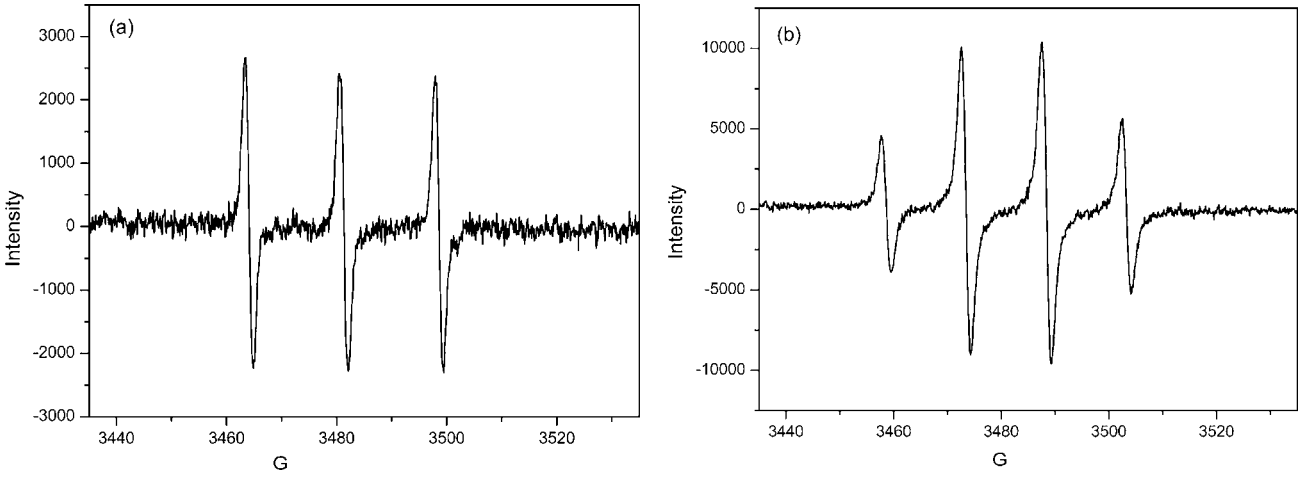

Fig. 6. ESR spectra of nitroxide radicals generated by reaction of the TEMP probe in $NaHCO_3$–H_2O_2–CdSe/CdS system (a), and ESR spectra of hydroxide radical addition to DMPO in $NaHCO_3$–H_2O_2 system (b). Conditions: (Receiver gain) 1.00e+05; (Modulation amplitude) 1G; (Sweep width) 100.00 G; (Microwave power) 1.00e+01 mW.

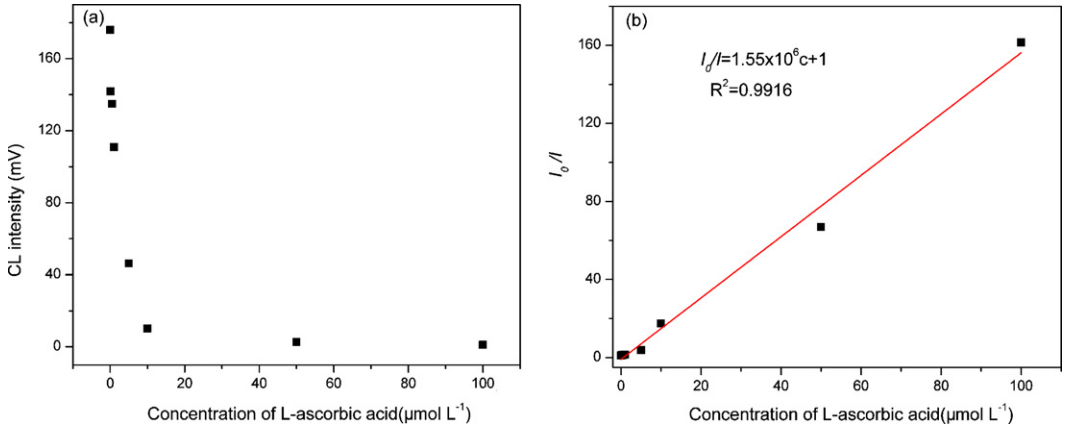

Fig. 7. Relationship between CL intensity and L-ascorbic acid concentration (a) and linear calibration plot for L-ascorbic acid (b). The solution conditions were 0.5 mol L^{-1} H_2O_2, 0.5 mol L^{-1} $NaHCO_3$, and 6.0×10^{-6} mol L^{-1} CdSe/CdS QDs.

(e^-_{1Se}) QDs and CdSe/CdS(h^+_{1Sh}) QDs for direct electron-hole recombination produced the excited CdSe/CdS QDs. The CL emission occurred when CdSe/CdS* QDs returned to the ground-state [38,39]. In HCO_3^-–H_2O_2–CdSe/CdS system, reactions of $^\bullet O_2^-$ and $^\bullet$OH radicals with CdSe/CdS QDs played important roles. The formation of $^1O_2$ and $(CO_2)_2^*$ were competed with the generation of CdSe/CdS* QDs. The CL intensity significantly depended on the rates of generation and annihilation of CdSe/CdS* QDs.

Room-temperature electron spin resonance (ESR) spectroscopy has been used to detect these free radical intermediates (Fig. 6a and b) [40]. 2,2,6,6-Tetramethyl-4-piperidine (TEMP) is a specific target molecule of $^1O_2$. It can react with $^1O_2$ to give the adduct-2,2,6,6-tetramethyl-4-piperidine-*N*-oxide (TEMPO), which is a stable nitroxide radical with a characteristic spectrum. Fig. 6a showed the specific signals of TEMPO, which supported the formation of $^1O_2$ in $NaHCO_3$–H_2O_2–CdSe/CdS QDs system.

5,5-Dimethyl-1-pyrroline *N*-oxide (DMPO)-a specific target molecule of $^\bullet$OH also was used. Fig. 6b presented the production of DMPO-OH adduct in $NaHCO_3$–H_2O_2 CL system. It confirmed the generation of $^\bullet$OH. But when DMPO was added into the mixture solution of CdSe/CdS QDs, $NaHCO_3$ and H_2O_2, the ESR signal disappeared. This phenomenon further proved that $^\bullet$OH existed and reacted with CdSe/CdS QDs.

Based on these conclusions, mechanism of the CL reaction enhanced by CdSe/CdS QDs was summarized as follows (Reactions 3–15):

$$HCO_3^- + H_2O_2 \rightleftharpoons HCO_4^- + H_2O \quad (3)$$

$$HCO_4^- \rightarrow {}^\bullet CO_3^- + {}^\bullet OH \quad (4)$$

$$H_2O_2 + {}^\bullet CO_3^- \rightarrow HCO_3^- + HO_2^\bullet \quad (5)$$

$$HO_2^\bullet \rightarrow H^+ + {}^\bullet O_2^- \quad (6)$$

$$^\bullet O_2^- + {}^\bullet OH \rightarrow {}^1O_2 + OH^- \quad (7)$$

$$^1O_2 \rightarrow {}^3O_2 + h\nu \quad (8)$$

$$^\bullet OH + HCO_3^- \rightarrow OH^- + {}^\bullet HCO_3 \quad (9)$$

$$2{}^\bullet HCO_3 \rightarrow (CO_2)_2^* + H_2O_2 \quad (10)$$

$$(CO_2)_2^* \rightarrow 2CO_2 + h\nu \quad (11)$$

$$CdSe/CdS + {}^\bullet O_2^- \rightarrow CdSe/CdS(e^-_{1Se}) + O_2 \quad (12)$$

$$CdSe/CdS + {}^\bullet OH \rightarrow CdSe/CdS(h^+_{1Sh}) + OH^- \quad (13)$$

$$CdSe/CdS(e^-_{1Se}) + CdSe/CdS(h^+_{1Sh}) \rightarrow CdSe/CdS^* \quad (14)$$

$$CdSe/CdS^* \rightarrow CdSe/CdS + hv \quad (15)$$

3.7. Analytical performance

The ratio of the initial CL intensity I_0 of $NaHCO_3$–H_2O_2–CdSe/CdS QDs system to the CL intensity I at a given concentration of L-ascorbic acid, I_0/I, was proportional to the concentration of L-ascorbic acid. The L-ascorbic acid concentration dependence of the CL intensity was coincident to the fluorescence quenching described by a Stern–Volmer equation (Eq. (2′)):

$$\frac{I_0}{I} = 1 + K_{sv}[Q] \quad (2')$$

K_{sv} was found to be 1.55×10^6 mol^{-1} L. This large value provided a sensitive CL detection of L-ascorbic acid (Fig. 7a and b).

Under the optimized experimental conditions, the relative CL intensity decreased linearly in the concentration range of 1.0×10^{-7}–1.0×10^{-4} mol L^{-1} for L-ascorbic acid ($R^2 = 0.9916$) with detection limit of 6.7×10^{-9} mol L^{-1} at S/N ratio of 3. The relative standard deviation (RSD) of 10 parallel measurements (intra-assay) at 20 μmol L^{-1} L-ascorbic acid with one QDs in the CL system was 4.8%. The RSD of six parallel measurements (inter-assay) at 20 μmol L^{-1} L-ascorbic acid with six QDs in the CL system was 4.1%, and the RSD of reproducibility in 1 week was 5.3%. The results indicate that the proposed CL system has good linearity, relatively high sensitivity and precision and acceptable reproducibility.

3.8. Interference studies

The interference of foreign species in the determination of 7×10^{-6} mol L^{-1} ascorbic acid using the proposed method was examined. Most ions did not interfere with the determination of

Table 2
Assessment of the interference by metal ion and organic compounds in the CL method for ascorbic acid.

Species added	Mole ratio ($C_{species}/C_{AA}$)	Variation of the CL peak height (%)
K^+	5000	2.12
Cl^-	5000	2.12
PO_4^{3-}	800	−2.30
L-Glutamic acid	1500	4.21
Glycin	2000	−8.35
L-Aspartic acid	1500	3.28
L-Isoleucine	1500	−6.02
Stearic acid	200	1.53
Uric acid	20	1.20
Dopamine	20	2.25
L-Cysteine	25	1.57
D-Glucose	25	1.24

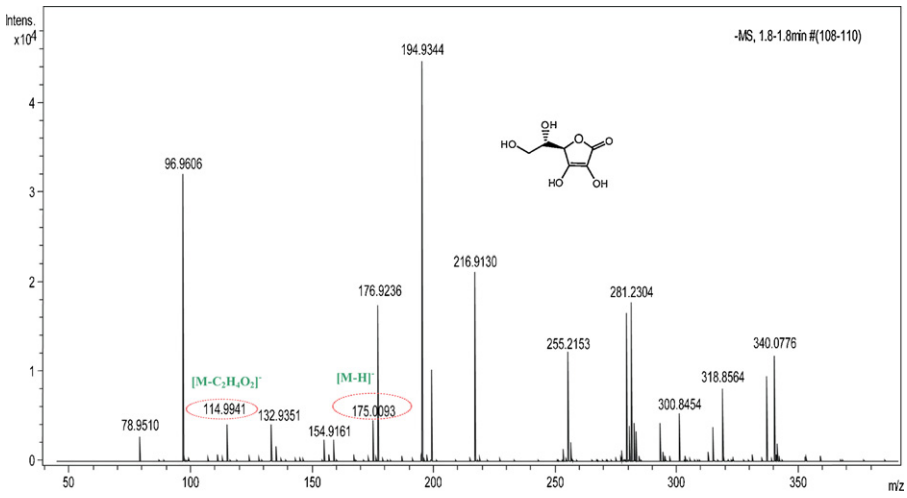

Fig. 8. Mass spectrum of human serum sample for L-ascorbic acid in negative ion model.

high concentration levels of L-ascorbic acid. Effects of some components of human serum, such as glycine, isoleucine, aspartic acid, glutamic acid and stearic acid were also investigated, and their interference could be excluded. Uric acid, dopamine, L-cysteine and D-glucose with the concentration beyond 0.2 mmol L^{-1} could affect and quench the CL. But their interferences could be neglected due to the low concentration in samples and the appropriate dilution. The results were summarized in Table 2, which demonstrated the high selectivity of the present method for the determination of L-ascorbic acid.

3.9. Application

The proposed method was applied to the determination of L-ascorbic acid in human serum. Samples were prepared as described in Section 2.4. Results showed that the coexisted substances in the samples did not interfere with the determination. Electrospray ionization quadrupole time-of-flight mass spectrometer (ESI-Q-TOF-MS) detection of L-ascorbic acid in these human serums was performed to confirm the method further (Fig. 8). The unprotonated molecular ion $[M-H]^-$ at m/z 175 was monitored at the mode of negative method. The characteristic fragment ion at m/z 115 originated from a direct elimination of $C_2H_4O_2$ from the parent ion.

Table 3
Results of L-ascorbic acid determination and recoveries in 6 human serum samples.

Sample no.	Added (μmol L^{-1})	Observed (μmol L^{-1})	Recovery (%)	RSD (n = 3, %)
1	0	14.00 ± 0.15	–	–
	5	18.91 ± 0.20	98	3.4
	10	22.95 ± 0.08	99	1.8
	20	35.79 ± 0.19	109	6.1
2	0	10.36 ± 0.16	–	–
	5	15.14 ± 0.17	96	2.4
	10	18.92 ± 0.17	86	3.0
	20	27.82 ± 0.19	87	4.8
3	0	24.92 ± 0.20	–	–
	10	35.16 ± 0.11	102	3.3
	20	46.46 ± 0.04	108	1.7
	40	68.99 ± 0.08	110	5.1
4	0	19.60 ± 0.17	–	–
	10	30.27 ± 0.22	107	5.9
	20	41.78 ± 0.10	111	3.7
	40	62.23 ± 0.06	107	3.4
5	0	32.20 ± 0.23	–	–
	15	47.32 ± 0.04	101	1.7
	30	64.72 ± 0.09	108	5.5
	60	91.60 ± 0.10	99	8.1
6	0	28.42 ± 0.26	–	–
	15	42.25 ± 0.10	92	3.8
	30	54.18 ± 0.12	86	5.8
	60	78.49 ± 0.02	83	1.4

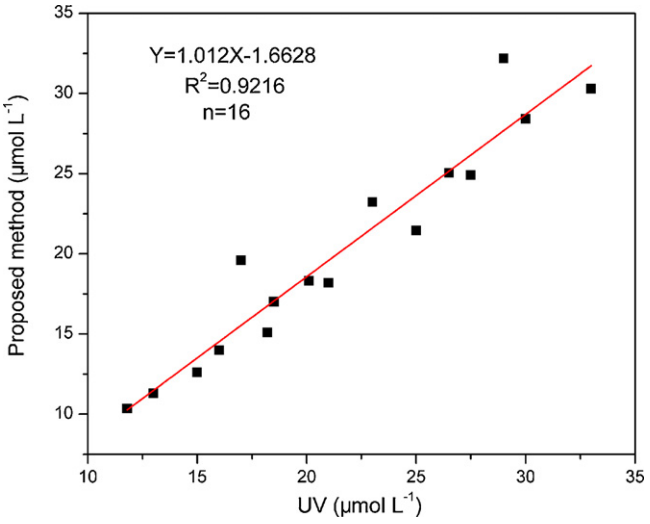

Fig. 9. Correlation between proposed method and UV method.

Recovery tests were performed to evaluate the accuracy of this method. Results for the contents and recoveries were summarized in Table 3. The recoveries ranged from 83% to 111%, with RSDs of <8.1%. It indicated that the proposed method was acceptable. Comparison between the presented FI-CL procedure and reported UV methods for the determination of L-ascorbic acid in 16 serum samples was performed. The regression line was Y (FIA-UV) = 1.012X – 1.6628, R^2 = 0.9216 (n = 16). The values correlated well, as shown in Fig. 9. The results were satisfactory and the proposed method was simple and direct.

4. Conclusion

A novel chemiluminescence system was established with $NaHCO_3$–H_2O_2 and CdSe/CdS QDs as the reagents. The mechanism of $NaHCO_3$–H_2O_2–CdSe/CdS QDs CL reaction was discussed.

The CL arose from the 1Se-1Sh transition emission. $\bullet O_2^-$ and •OH were key species in the CL process. The proposed CL system has good linearity, high sensitivity and precision and the method has been successfully applied to the determination of L-ascorbic acid in human serum.

Acknowledgement

This work was supported by National Natural Science Foundation of China (No. 20935002).

References

[1] M. Castro, T. Caprile, A. Astuya, C. Millan, K. Reinicke, J.C. Vera, O. Vasquez, L.G. Aguayo, F. Nualart, J. Neurochem. 78 (2001) 815.
[2] D. Njus, V. Jalukar, J. Zu, P.M. Kelley, Am. J. Clin. Nutr. 54 (1991) 1179.
[3] S.P. Arya, M. Mahajan, P. Jain, Anal. Chim. Acta 417 (2000) 1.
[4] H.-L. Liu, S.-P. Ou, Chin. J. Anal. Chem. 30 (2002) 122.
[5] Q.-L. Wang, Z.-H. Liu, L.-Y. Mao, R.-X. Cai, Chin. J. Anal. Chem. 28 (2000) 1229.
[6] P.L. Adriani, Anal. Biochem. 263 (1998) 176.
[7] A.G. Frenich, M.E.H. Torres, A.B. Vega, J.L.M. Vidal, P.P. Bolaños, J. Agric. Food Chem. 53 (2005) 7371.
[8] R. Shakya, D.A. Navarre, J. Agric. Food Chem. 54 (2006) 5253.
[9] J. Oni, P. Westbroek, T. Nyokong, Electroanalysis 15 (2003) 847.
[10] M. Tabata, H. Morita, Talanta 44 (1997) 151.
[11] F. Li, G.-Y. Zhu, Chin. J. Anal. Chem. 30 (2002) 580.
[12] C. Zhu, L. Wang, J. Wu, Chin. J. Anal. Lab. 15 (1996) 49.
[13] A. Sheng, B. Xu, M. Ji, J. Wu, J. Anal. Sci. 13 (1997) 347.
[14] Z. Zhang, H. Cui, C.-Z. Lai, L.-J. Liu, Anal. Chem. 77 (2005) 3324.
[15] J. Perroy, S. Pontier, P.G. Charest, M. Aubry, M. Bouvier, Nat. Methods 1 (2004) 203.
[16] X. Michalet, F.F. Pinaud, L.A. Bentolila, J.M. Tsay, S. Doose, J.J. Li, G. Sundaresan, A.M. Wu, S.S. Gambhir, S. Weiss, Science 307 (2005) 538.
[17] W.C.W. Chan, S.M. Nie, Science 281 (1998) 2016.
[18] Z. Wang, J. Li, B. Liu, J. Hu, X. Yao, J. Li, J. Phys. Chem. B 109 (2005) 23304.
[19] H.R. Yao, D.E. Richardson, J. Am. Chem. Soc. 125 (2003) 6211.
[20] X.-G. Su, Z.-B. Lin, H. Hu, J.-H. Zhang, Q.-H. Jin, Chem. Res. Chinese U 3 (2003) 269.
[21] W.W. Yu, L.H. Qu, W.Z. Guo, X.G. Peng, Chem. Mater. 15 (2003) 2854.
[22] A.-L. Rogach, D. Nagesha, J.-W. Ostrander, M. Giersig, N.-A. Kotov, Chem. Mater. 12 (2000) 2676.
[23] J.N. Demas, G.A. Crosby, J. Phys. Chem. 75 (1971) 991.
[24] C. Liu, L. Jiang, D. Zheng, Y. Li, G. Lu, Chin. J. Anal. Chem. 33 (2005) 1171.
[25] Z. Dai, H.X. Ju, Phys. Chem. Chem. Phys. 3 (2001) 3769.
[26] H.F. Cordes, H.P. Richter, C.A. Heller, J. Am. Chem. Soc. 91 (1969) 7209.
[27] L.J. Bollyky, J. Am. Chem. Soc. 92 (1970) 3230.
[28] C. Lu, J.-M. Lin, Catal. Today 90 (2004) 343.
[29] A.-U. Khan, M.J. Kasha, Chem. Phys. 39 (1963) 2105.
[30] D.E. Richardson, H.R. Yao, K.M. Frank, D.A. Bennett, J. Am. Chem. Soc. 122 (2000) 1729.
[31] M. Liu, L. Zhao, J.-M. Lin, J. Phys. Chem. A 110 (2006) 7509.
[32] M. Liu, X. Cheng, L. Zhao, J.-M. Lin, Luminescence 21 (2006) 179.
[33] S. Liang, L. Zhao, B. Zhang, J.-M. Lin, J. Phys. Chem. A 112 (2008) 618.
[34] J.-M. Lin, M. Liu, J. Phys. Chem. B 112 (2008) 7850.
[35] B.H.J. Bielski, D.E. Cabelli, R.L. Arudi, A.B. Ross, J. Phys. Chem. Ref. Data 14 (1985) 1041.
[36] A.U. Khan, M. Kasha, J. Am. Chem. Soc. 92 (1970) 3293.
[37] W.H. Koppenol, J.J. Moreno, W.A. Pryor, H. Ischiropoilos, J.S. Beckman, Chem. Res. Toxicol. 5 (1992) 834.
[38] X. Liu, H. Jiang, J. Lei, H. Ju, Anal. Chem. 79 (2007) 8055.
[39] Y. Sawada, T. Iyanagi, I. Yamazaki, Biochemistry 14 (1975) 3761.
[40] F. Villamena, E. Locigno, A. Rockenbauer, C. Hadad, J. Zweier, J. Phys. Chem. A 111 (2007) 384.